Indian Journal of Pharmaceutical Education and Research | Association of Pharmaceutical Teachers of India

Pharmaceutical Eutectic and Non-eutectic Alloys of Nicotinamide-2-methylimidazole System: Thermodynamic and Interfacial Studies

Shekhar H* and Kant Vishnu

Department of Chemistry, V. K. S. University, Ara, 802301, India

ABSTRACT

Submitted: 09/07/2012 *Accepted: 28/03/2013*

The solid-liquid equilibrium phase diagram of Nicotinamide (NA)- 2-Methylimidazole(MIM) system in form of temperature-composition curve determined by Thaw- melt method, suggests the formation of simple eutectic(E) at 102°C and at 0.451 mole fraction of MIM. The excess thermodynamic quantities have been determined by computing heat of fusion data and activity coefficient of the component in binary mix. These values highlight the ordering, stability and structure of eutectic and non-eutectic alloys. The thermodynamic mixing functions describe about the nature of mixing of the components during alloying. The Gibb's-Duhem equations give the graphical solution of activity, activity coefficient and partial mixing thermodynamic quantities.

Keywords: Nicotinamide, Phase diagram, Thermodynamic excess and mixing functions, stability factors

INTRODUCTION

Nicotinamide is water soluble vitamin. It has an anti inflammatory effect. It lacks the vasodilator, gastrointestinal, hepatic and hypolipemic action of niacin. As such nicotinamide has not been shown to produce the flushing, itching and burning sensations of the skin as is commonly seen when large doses of niacin are administrated orally[1,2]. Nicotinamide, a derivative of the B vitamin niacin, is currently under trial for the prevention of insulin-dependent diabetes mellitus after success in the NOD mouse. Nicotinamide has been used as a treatment for *M. tuberculosis* faded rapidly when one of the foremost research groups of the day reported antagonism between nicotinamide and isoniazid when they were used together as a binary drug therapeutic regimen[3,4]. In fact, a comprehensive review of nicotinamide's pharmaceutical effects came in light in 1991 as anti HIV agent[5] and after that popularized vastly. 2-Methylimidazole(MIM) is intermediate/starting materials or components in the manufacture of pharmaceuticals, photographic and photothermographic chemicals, dyes and pigments, agricultural chemicals, and rubber; these chemicals have been identified as undesirable by-products in several foods and have been detected in mainstream and sidestream tobacco smoke. 2-Methylimidazole is widely used as a polymerization crosslinking accelerator and hardner for epoxy resin systems for semiconductor potting compounds and soldering masks. It is a component of numerous polymers, including epoxy resin pastes, acrylic rubber-fluororubber laminates, films, adhesives, textile finishes, and epoxy silane coatings. It is also used as a dyeing auxiliary for acrylic fibers and plastic foams. Imidazole nucleus has proved to be an abundant source for a number of medicinal agents and associated with many activities viz, antiprotozoal, mutagenic properties, anticancer, antiviral, muscarinic anticholingergic activity enzyme inhibition, H2-Antagonism, α-Adrenergic agonist and β-blocking, anticonvulsant, broad spectrum antibacterial, Antispasmodic activity and antifungal activities[6-8]. Eutectic mixture formation between nicotinamide based drugs and hydrophilic carriers was investigated[9] recently to reduce the drug particle size, and increases the dissolution rate and thus changes the biopharmaceutical properties. In the present study pharmaceutical active Nicotinamide (NA)-2-Methylimidazole (MIM) drug system was selected for the solid-liquid equilibrium phase diagrm, thermodynamic and interfacial investigations of eutectic and non-eutectic drug alloys.

***Address for Correspondence:**
Shekhar H, Department of Chemistry, V. K. S. University, Ara, 802301, India
E-mail: hshe2503@rediffmail.com

Experimental procedure

Nicotinamide (Thomas Baker, Bombey), 2-Methylimidazole (G.S. Chemical, India) were directly taken for investigation. The melting point (experimental value) of nicotinamide, 2-methylimidazole was found to be 128°C and 143°C respectively. The solid-liquid equilibrium data of NA-MIM system was determined by the Thaw-melt method[10-11]. Mixtures of different composition were made in glass test tubes by repeated heating and followed by chilling in ice. The melting and thaw temperatures were determined in a Toshniwal melting point apparatus using a precision thermometer which could read correctly up to ± 0.1°C. The heater was regulated to give above 1°C increase in temperature in every five minutes.

Heat of fusion of materials was measured by the DTA method[12-13] using NETZSCH Simultaneous Thermal Analyzer, STA 409 series unit. All the runs were carried out with heating rate 2°C/min, chart speed 10mm/min and chart sensitivity 100μv/10mv.The sample weight was 5 mg for all estimation. Using benzoic acid was a standard substance, the heat of fusion of unknown compound was determined using the following equation:

$$\Delta H_x = \frac{\Delta H_s W_s A_x}{W_x A_s}$$

where, ΔH_x is the heat of fusion of unknown sample and ΔH_s is the heat of fusion of standard substance. W and A are weight and peak area, respectively and suffices x and s indicate the corresponding quantities for the unknown and standard substances, respectively.

RESULTS AND DISCUSSION

Phase Diagram

The solid-liquid equilibrium phase diagram of NA-MIM system determined by the thaw melt method, is reported in the form of temperature-composition curve (Fig.1). NA-MIM system shows the formation of simple eutectic. Eutectic of NA-MIM is formed at 102°C and 0.451 mole fraction of MIM. The melting point of NA (128°C) decreases on the addition of second component MIM (M.P., 143°C) and further attains minimum and then increases. At the eutectic temperature two phases namely a liquid phase L and two solid phases (S_1 and S_2) are in equilibrium and the system is invariant. In the region indicated by L a homogenous binary liquid solution exists while the two solid phases exists below the horizontal line. In the case, in region located on the left side of the diagram a binary liquid and solid NA exist while in a similar region located on the right side of the diagram a binary liquid and the second component of the system co-exist.

$$L \xrightleftharpoons{\text{Cooling}} S_1 + S_2$$

The chemical interaction between two components in a binary system leads to an association of molecules in definite quantities. Physical as well as chemical forces are involved in the formation of eutectic and non-eutectic alloys. Thermodynamical studies unfold the nature of mixing as well as nature of interaction between components during binary mix.

Heat of Fusion

The values of heats of fusion of eutectic and noneutectic alloys are calculated by the mixture law using equation

$$(\Delta H)_e = \chi_{NA}\,\Delta H_{NA} + \chi_{MIM}\,\Delta H_{MIM} \quad \text{..... (1)}$$

where x and ΔH are the mole fraction and the heat of fusion of the component indicated by the subscript, respectively. The value of heat of fusion of binary alloys A_1-A_{14}, E is reported in Table 1.

Activity and Activity Coefficient

The activity coefficient of components for the systems under investigation has been calculated from the equation[14] given below

$$-\ln\chi_i^1\gamma_i^1 = \frac{\Delta H_i}{R}\left(\frac{1}{T_e} - \frac{1}{T_i}\right) \quad \text{..... (2)}$$

where γ_i^1 is activity coefficient of the component *i* in the liquid phase respectively, ΔH_i is the heat of fusion of component i at melting point T_i and R is the gas constant. T_e is the melting temperature of alloy. Using the values of activity and activity coefficient (Table 1) of the components in alloys mixing and excess thermodynamics functions have been computed.

Mixing Functions

Integral molar free energy of mixing (ΔG^M), molar entropy of mixing (ΔS^M) and molar enthalpy of mixing (ΔH^M) and partial thermodynamic mixing functions of the binary alloys when two components are mixed together were determined by using the following equations

$$\Delta G^M = RT(\chi_{NA}\ln a_{NA} + \chi_{MIM}\ln a_{MIM}) \quad \text{..... (3)}$$

$$\Delta S^M = R(\chi_{NA}\ln\chi_{NA} + \chi_{MIM}\ln\chi_{MIM}) \quad \text{..... (4)}$$

$$\Delta H^M = RT(\chi_{NA}\ln\gamma_{NA} + \chi_{MIM}\ln\gamma_{MIM}) \quad \text{..... (5)}$$

$$G_i^M = \mu_i^M = RT\ln a_i \quad \text{..... (6)}$$

where G_i^M (μ_i^M) is the partial molar free energy of mixing of component i (mixing chemical potential)in binary mix. and γ_i and a_i is the activity coefficient and activity of component respectively. The negative value[15,16] of molar free energy of mixing of alloys (A_4-A_8, E and A_9-A_{14}) (Table 2) suggests that the mixing in all cases is spontaneous. The integral molar enthalpy of mixing value corresponds to the value of excess integral molar free energy of the system favors the regularity in the binary solutions.

Excess Thermodynamic Functions

In order to unfold the nature of the interactions between the components forming the eutectic, noneutectic alloys and addition compound, the excess thermodynamic functions such as integral excess integral free energy (g^E), excess integral entropy (s^E) and excess integral enthalpy (h^E) were calculated using the following equations)

$$g^E = RT(\chi_{NA} \ln \gamma_{NA} + \chi_{MIM} \ln \gamma_{MIM}) \quad \text{..... (7)}$$

$$s^E = R\left(\chi_{NA} \ln \gamma_{NA} + \chi_{MIM} \ln \gamma_{MIM} + \chi_{NA} T \frac{\delta \ln \gamma_{NA}}{\delta T} + \chi_{MIM} T \frac{\delta \ln \gamma_{MIM}}{\delta T}\right) \quad \text{..... (8)}$$

$$h^E = RT^2 \left(\chi_{NA} \frac{\delta \ln \gamma_{NA}}{\delta T} + \chi_{MIM} \frac{\delta \ln \gamma_{MIM}}{\delta T}\right) \quad \text{..... (9)}$$

and excess chemical potential or excess partial free energy of mixing

$$g_i^E = \mu_i^M = RT \ln \gamma_i \quad \text{..... (10)}$$

The values of $d\ln g_i / dT$ can be determined by the slope of liquidus curve near the alloys form in the phase diagram. The values of the excess thermodynamic functions are given in Table 3. The value of the excess free energy is a measure of the departure of the system from ideal behavior. The reported excess thermodynamic data substantiate the earlier conclusion of an appreciable interaction between the parent components during the formation of alloys. The positive value[17,18] of excess free energy for all the eutectic and non-eutectic alloys indicates the possibility of a stronger association between like molecules. The excess entropy is a measure of the change in configurational energy due to a change in potential energy and indicates an increase in randomness.

Gibbs-Duhem Equation

Further the partial molar quantity, activity and activity coefficient can also be determined by using Gibbs-Duhem equation

$$\sum \chi_i d\bar{z}_i^M = 0 \quad \text{..... (11)}$$

$$or\ \chi_{NA} d\bar{H}_{NA}^M + \chi_{MIM} d\bar{H}_{MIM}^M = 0 \quad \text{..... (12)}$$

$$or\ d\bar{H}_{NA}^M = \frac{\chi_{MIM}}{\chi_{NA}} d\bar{H}_{MIM}^M \quad \text{..... (13)}$$

$$or\ \left[\bar{H}_{NA}^M\right]_{\chi_{NA}=y} = \int_{\chi_{NA}=y}^{\chi_{NA}=1} \frac{\chi_{MIM}}{\chi_{NA}} d\bar{H}_{MIM}^M \quad \text{..... (14)}$$

Using equation (14) a graph between $\bar{H}_{MIM}^M$ and χ_{MIM}/χ_{NA} gives the solution of the partial molar heat of mixing of a constituent NA in NA/MIM alloy and plot between χ_{MIM}/χ_{NA} vs $\ln g_{MIM}$ determines the value of activity coefficient of component NA in binary alloys.

Interface Morphology

The science of growth has been developed on the foundation of thermodynamics, kinetics, fluid dynamics, crystal structures and interfacial sciences. The solid-liquid interface morphology can be predicted from the value of the entropy of fusion. According to Hunt and Jackson[19], the type of growth from a binary melt depends upon a factor α, defined as:

$$\alpha = \xi \frac{\Delta H}{RT} = \xi \frac{\Delta S}{R} \quad \text{..... (15)}$$

where x is a crystallographic factor depending upon the geometry of the molecules and has a value less than or equal to one. ΔS/R (also known as Jackson's roughness parameter α) is the entropy of fusion (dimensionless) and R is the gas constant. When α is less than two the solid-liquid interface is atomically rough and exhibits non-faceted growth. The value of Jackson's roughness parameter (ΔS/R) is given in Table 1. For the entire alloy the α value was found greater than 2 which indicate the faceted growth proceeds in all the cases.

The Solid-Liquid Interfacial Energy (σ)

It has been found that an experimentally observed value of interfacial energy 'σ' keeps a variation of 50-100% from one worker to other. However, Singh and Glickman[20] were calculated the solid-liquid interfacial energy (σ) from melting enthalpy change and values obtained are found in good agreement with the experimental values. Turnbull empirical relationship[21] between the interfacial energy and enthalpy change provides the clue to determine the interfacial energy value of alloy and is expressed as:

$$\sigma = \frac{C\Delta H}{(N)^{1/3}(V_m)^{2/3}} \quad \text{..... (16)}$$

where the coefficient *C* lies between 0.33 to 0.35 for nonmetallic system, V_m is molar volume and N is the Avogadro's constant. The value of the solid-liquid interfacial energy of nicotinamide and 2-methylimidazole was found to be 5.046 x 10^{-02} and 2.484 x 10^{-02} J m^{-2} respectively and σ value of alloys was given in Table 1.

The effective entropy change (ΔS$_v$)

It is obvious that the effective entropy change and the volume fraction of phases in the alloy are inter-related to decide the

interface morphology during solidification and the volume fraction of the two phases depends on the ratio of effective entropy change of the phases. The entropy of fusion (S = H/T) value (Table 1) of alloys is calculated by heat of fusion values of the materials. The effective entropy change per unit volume (ΔS_V) is given by

$$\Delta S_v = \frac{\Delta H}{T} \cdot \frac{1}{V_m} \quad \text{..... (17)}$$

where ΔH is the enthalpy change, T is the melting temperature and V_m is the molar volume of solid phase. The entropy of fusion per unit volume (ΔS_V) for NA and MIM was found 726 and 342 $kJK^{-1}m^{-3}$ respectively. Values of ΔS_V for alloys are reported in Table 1.

The Driving Force of Nucleation (ΔG_v)

During growth of crystalline solid there is change in enthalpy, entropy and specific volume and non-equilibrium leads Gibb's energy. Thermodynamically metastable phase occurs in a supersaturated or super-cooled liquid. The driving force for liquid-solid transition is the difference in Gibb's energy between the two phases. The theories of solidification process in past have been discussed on the basis of diffusion model, kinetic characteristics of nucleation and on thermodynamic features. The lateral motion of rudementry steps in liquid advances stepwise/ non-uniform surface at low driving force while continuous and uniform surface advances at sufficiently high driving force. The driving force of nucleation from liquid to solid during solidification (ΔG_V) can be determined at different undercoolings (T) by using the following equation.[22]

$$\Delta G_v = S_v T \quad \text{..... (18)}$$

It is opposed by the increase in surface free energy due to creation of a new solid-liquid interface. By assuming that solid phase nucleates as small spherical cluster of radius arising due to random motion of atoms within liquid. The value of ΔG_V for alloys and pure components are shown in the Table 4.

The Critical Radius (r*)

During liquid-solid transformation embryos are rapidly dispersed in unsaturated liquid and on undercooling liquid becomes saturated and provide embryo of a critical size with radius r* for nucleation which can be expressed by the Chadwick relation.[23]

$$r^* = \frac{2\sigma}{\Delta G_v} = \frac{2\sigma T}{\Delta H_v \Delta T} \quad \text{..... (19)}$$

where σ is the interfacial energy and ΔH_V is the enthalpy of fusion of the compound per unit volume, respectively. The critical size of the nucleus for the components and alloys was calculated at different undercoolings and values are presented in Table 5. It can be inferred from table that the size of the critical nucleus decreases with increase in the undercooling of the melt. The existence of embryo and a range of embryo size can be expected in the liquid at any temperature.

Critical Free Energy of Nucleation (G*)

To form critical nucleus, it requires a localized critical free energy of nucleation (G*) which is evaluated[24] as

$$\Delta G^* = \frac{16}{3} \frac{\pi \sigma^3}{\Delta G_v^2} \quad \text{..... (20)}$$

The value of G* for alloys and pure components has been found in the range of 10^{-15} to 10^{-16} J at different undercoolings, and has been reported in Table 6.

Gibbs-Thomson Coefficient (τ)

For a planar grain boundary on planar solid-liquid interface the Gibbs-Thomson coefficient (τ) for the system can be calculated by the Gibbs-Thomson equation is expressed as

$$\tau = r\Delta T = \frac{TV_m\sigma}{\Delta H} = \frac{\sigma}{\Delta S_v} \quad \text{..... (21)}$$

where τ is the Gibbs-Thomson coefficient, ΔT is the dispersion in equilibrium temperature and, r is the radius of grooves of interface. The theoretical basis of determination of τ was made for equal thermal conductivities of solid and liquid phases for some transparent materials. It was also determined by the help of Gunduz and Hunt numerical method[25] for materials having known grain boundary shape, temperature gradient in solid and the ratio of thermal conductivity of the equilibrated liquid phases to solid phase ($R = K_L/K_S$).The Gibbs-Thomson coefficient for NA, MIM is 1.343 – 1.402 x 10^{-05} Km respectively and their alloys are found in the range of 1.269 – 1.402 x 10^{-05} Km and is reported in Table 1.

Interfacial Grain Boundary Energy (σ_{gb})

Grain boundary is the internal surface which can be understood in a very similar way to nucleation on surfaces in liquid-solid transformation. In past, a numerical method[26] is applied to observe the interfacial grain boundary energy (σ_{gb}) without applying the temperature gradient for the grain boundary groove shape. For isotropic interface there is no difference in the value of interfacial tension and interfacial energy. A considerable force is employed at the grain

Table 1 : Phase Composition, Melting Temperature, Values of Enthalpy of Fusion(ΔH), Entropy of Fusion (ΔS) and Roughness Parameter(α)

Alloy	χ_{NA}	MP(°C)	DH (kJ/mol)	DS (J/mol/K)	g_{NA}	g_{MIM}
A1	0.930	137	24.51	59.78	1.27	14.96
A2	0.856	131	23.57	58.33	1.24	6.88
A3	0.776	129	22.55	56.09	1.31	4.341
A4	0.690	120	21.45	54.59	1.24	2.876
A5	0.645	118	20.88	53.40	1.28	2.462
A6	0.617	112	20.52	53.31	1.18	2.147
A7	0.598	108	20.28	53.24	1.12	1.963
A8	0.579	107	20.04	52.74	1.13	1.854
E	0.549	102	19.66	52.42	1.07	1.641
A9	0.498	105	19.01	50.29	1.26	1.523
A10	0.477	105	18.74	49.58	1.32	1.461
A11	0.455	106	18.46	48.71	1.41	1.417
A12	0.389	108	17.62	46.25	1.72	1.291
A13	0.271	118	16.12	41.23	3.04	1.199
A14	0.142	123	14.48	36.56	6.40	1.07

Table 2: Value of Partial And Integral Mixing of Gibbs Free Energy(DG^M), Enthalpy(DH^M) And Entropy(DS^M) of NA-MIM System

Alloy	DG_{NA}^{-M} J/mol	DG_{MIM}^{-M} J/mol	DG^M J/mol	DH_{NA}^{-M} J/mol	DH_{MIM}^{-M} J/mol	DH^M J/mol	DS_{NA}^{-M} J/mol/K	DS_{MIM}^{-M} J/mol/K	DS^M J/mol/K
A	1570.07	156.42	541.128	17.45	9221.15	-1405.71	0.60	22.11	2.11
A2	190.02	-31.28	158.16	712.28	6477.98	-1542.54	1.29	16.11	3.43
A3	63.34	-93.85	28.13	910.94	4906.49	-1805.94	2.11	12.44	4.42
A4	-506.73	-375.41	-466.02	705.68	3451.32	-1556.83	3.09	9.74	5.15
A5	-633.42	-437.98	-564.04	792.06	2928.65	-1550.55	3.65	8.61	5.41
A6	-1013.47	-625.68	-864.94	532.20	2446.28	-1265.29	4.02	7.98	5.53
A7	-1266.83	-750.82	-1059.39	361.85	2135.86	-1075.00	4.28	7.58	5.60
A8	-1330.17	-782.10	-1099.43	396.24	1951.10	-1050.84	4.54	7.19	5.66
E	-1646.88	-938.52	-1327.41	222.70	1544.11	-818.65	4.99	6.62	5.72
A9	-1456.86	-844.67	-1149.54	734.09	1321.14	-1028.79	5.80	5.73	5.76
A10	-1456.86	-844.67	-1136.68	869.48	1192.34	-1038.34	6.15	5.39	5.75
A11	-1393.52	-813.38	-1077.34	1087.77	1099.18	-1093.99	6.55	5.05	5.73
A12	-1266.83	-750.82	-951.55	1723.97	809.75	-1165.38	7.85	4.10	5.56
A13	-633.42	-437.98	-490.94	3610.91	589.53	-1408.33	10.86	2.6	34.86
A14	-316.71	-281.56	-286.55	6109.71	222.67	-1058.63	16.23	1.27	3.40

Table 3: Value of Partial and Integral Excess Gibbs Free Energy(g^E), Enthalpy(h^E) and Entropy(s^E) Of NA-MIM System

Alloy	g_{NA}^{-E} J/mol	g_{MIM}^{-E} J/mol	g^E J/mol	h_{NA}^{-E} J/mol	h_{MIM}^{-E} J/mol	h^E J/mol	s_{NA}^{-E} J/mol/K	s_{MIM}^{-E} J/mol/K	ss^E J/mol/K
A1	817.45	9221.15	1405.71	-10372.22	186984.77	3442.77	-27.29	433.57	4.97
A2	712.28	6477.98	1542.54	6305.09	175799.14	30712.23	13.84	419.11	72.20
A3	910.94	4906.49	1805.94	-8085.88	47311.06	4323.03	-22.38	105.48	6.26
A4	705.68	3451.32	1556.83	2514.98	49463.34	17068.97	4.60	117.08	39.47
A5	792.06	2928.65	1550.55	-5693.76	23134.30	4540.20	-16.59	51.68	7.65
A6	532.20	2446.28	1265.29	-15413.43	3418.02	-8200.98	-41.42	2.52	-24.59
A7	361.85	2135.86	1075.00	-11878.23	7444.48	-4110.50	-32.13	13.93	-13.61
A8	396.24	1951.10	1050.84	16069.49	44362.86	27980.99	41.25	111.61	70.87
E	222.70	1544.11	818.654	-14751.95	291.82	-7967.21	-39.93	-3.34	-23.43
A9	734.09	1321.14	1028.79	46162.50	58322.29	52266.71	120.18	150.80	135.55
A10	869.48	1192.34	1038.34	49313.06	55471.74	52534.04	128.16	143.60	136.23
A11	1087.80	1099.18	1093.99	499536.80	425580.01	459230.40	1315.25	1120.04	1208.84
A12	1724.00	809.75	1165.38	21137.35	16958.52	18584.09	0.95	2.39	5.72
A13	3610.90	589.53	1408.33	44953.47	13483.35	22011.75	105.74	32.98	52.69
A14	6109.70	222.67	1058.63	66414.66	2525.43	11597.70	152.29	5.82	26.61

Table 4: Critical Size Of Nucleus (r*) At Different Undercoolings (∆t)

Alloy	r*(cm) x 10^5					
∆T	1.0	1.5	2.0	2.5	3.0	3.5
A1	1.422	2.133	2.844	3.554	4.265	4.976
A2	1.402	2.102	2.803	3.504	4.205	4.906
A3	1.395	2.093	2.791	3.489	4.186	4.884
A4	1.365	2.048	2.730	3.413	4.095	4.778
A5	1.358	2.038	2.718	3.396	4.075	4.755
A6	1.338	2.007	2.676	3.345	4.014	4.683
A7	1.324	1.986	2.648	3.310	3.972	4.635
A8	1.321	1.981	2.642	3.302	3.963	4.623
E	1.304	1.956	2.607	3.259	3.911	4.563
A9	1.315	1.972	2.629	3.286	3.944	4.601
A10	1.315	1.972	2.630	3.287	3.944	4.602
A11	1.318	1.978	2.637	3.296	3.955	4.615
A12	1.326	1.989	2.652	3.315	3.978	4.641
A13	1.397	2.095	2.793	3.492	4.190	4.888
A14	1.398	2.097	2.796	3.495	4.194	4.893
NA	1.390	2.085	2.780	3.475	4.170	4.865
MIM	1.399	2.099	2.798	3.498	4.198	4.897

Table 5: Value of Volume Free Energy Change (ΔG_v) during Solidification for NA-MIN System at Different Undercoolings (∆T)

Alloy	DG_v (J/cm^3)					
∆T	1.0	1.5	2.0	2.5	3.0	3.5
A1	0.684	1.026	1.369	1.711	2.053	2.395
A2	0.667	1.000	1.334	1.667	2.000	2.334
A3	0.640	0.960	1.280	1.600	1.920	2.240
A4	0.622	0.933	1.244	1.555	1.866	2.177
A5	0.608	0.912	1.216	1.52	1.823	2.127
A6	0.606	0.910	1.213	1.516	1.819	2.122
A7	0.605	0.908	1.211	1.513	1.816	2.119
A8	0.599	0.899	1.199	1.499	1.798	2.098
E	0.596	0.893	1.191	1.489	1.787	2.084
A9	0.571	0.856	1.141	1.427	1.712	1.997
A10	0.562	0.844	1.125	1.406	1.687	1.968
A11	0.552	0.828	1.105	1.381	1.657	1.933
A12	0.524	0.786	1.047	1.309	1.571	1.833
A13	0.466	0.699	0.931	1.164	1.397	1.63
A14	0.412	0.618	0.824	1.030	1.236	1.442
NA	0.726	1.089	1.452	1.815	2.178	2.541
MIM	0.342	0.513	0.684	0.856	1.027	1.198

Table 6: Value of Critical Free Energy of Nucleation (ΔG*) for Alloys of NA - MIM System at Different Undercooling (ΔT)

Alloy	ΔG*(J/mol) x 10^{15}					
ΔT	1.0	1.5	2.0	2.5	3.0	3.5
A1	4.12	1.83	1.03	0.66	0.458	0.336
A2	3.85	1.71	0.96	0.62	0.427	0.314
A3	3.64	1.70	0.91	0.58	0.405	0.297
A4	3.31	1.47	0.83	0.53	0.368	0.271
A5	3.19	1.50	0.80	0.51	0.355	0.261
A6	3.04	1.35	0.76	0.49	0.338	0.248
A7	2.94	1.31	0.74	0.47	0.327	0.240
A8	2.89	1.29	0.72	0.46	0.322	0.236
E	2.76	1.23	0.69	0.44	0.307	0.226
A9	2.72	1.21	0.68	0.43	0.302	0.222
A10	2.68	1.19	0.67	0.43	0.298	0.219
A11	2.65	1.18	0.66	0.42	0.295	0.217
A12	2.56	1.14	0.64	0.41	0.284	0.209
A13	2.46	1.10	0.62	0.39	0.274	0.201
A14	2.27	1.01	0.57	0.36	0.252	0.185
NA	4.08	1.82	1.02	0.65	0.454	0.333
MIM	2.19	9.75	0.55	0.35	0.244	0.179

Fig. 1: Phase diagram of Nicotinamide-2-methylimidazole system

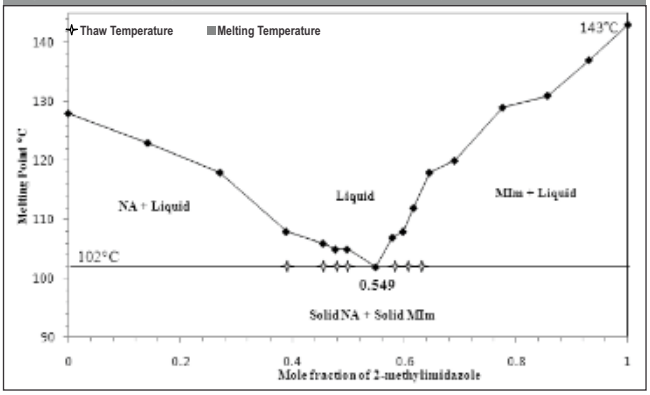

Fig. 2: Graphical solution of partial molar enthalpy of mixing in binary mix

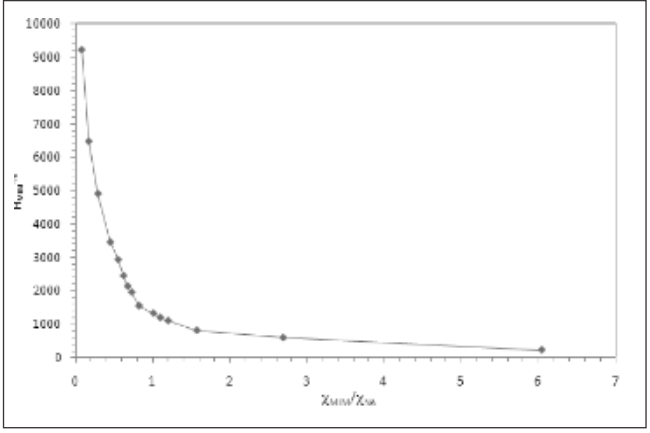

Fig. 3: Graphical solution of activity coefficient of a specific component in the binary mix

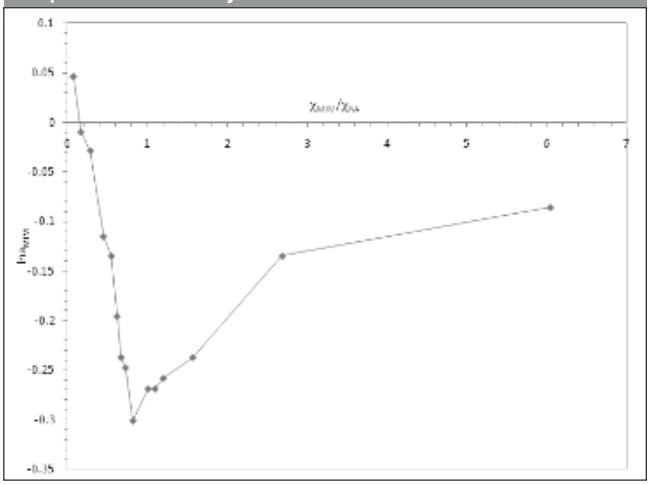

boundary groove in anisotropic interface. The grain boundary energy can be obtained by the equation:

$$\sigma_{gb} = 2\sigma\cos\theta \quad \text{..... (22)}$$

where θ is equilibrium contact angle precipitates at solid-liquid interface of grain boundary. The grain boundary energy could be twice the solid-liquid interfacial energy in the case where the contact angle tends to zero. The value of σ_{gb} for solid NA and MIM was found to be 9.748 x 10^{-2} and 4.798 x 10^{-2} Jm^{-2} respectively and the value for all alloys is given in Table 1.

CONCLUSIONS

The solid-liquid equilibria of the systems NA-MIM infer the formation of simple eutectic. The mixing function suggests the spontaneous mixing overall the alloys of the system while excess functions describe the stronger association between the same components in the binary melt. Jackson's Interface roughness (α > 2) predicts the faceted growth leads in all the eutectic and non-eutectic alloys.

ACKNOWLEDGEMENT

Thanks are due to the Head Department of Chemistry, V K S University Ara 802301, India for providing research facilities. We are also thankful to UGC New Delhi for financial support.

REFERENCES

1. Knip M, Douek IF and Moore WP. Safety of high-dose nicotinamide: a review, Diabetologia 2000; 43: 1337.
2. Hakozaki T, Minwalla L and Zhung J. The effect of niacinamide on reducing cutaneous pigmentation and suppression of melanosome transfer, *Br.* J. Dermatol 2002; 147: 20.

3. Murray Michael F., Nicotinamide: An Oral Antimicrobial Agent with Activity against Both Mycobacterium tuberculosis and Human Immunodeficiency Virus, Clinical Infectious Diseases, 2003, 36, 453-60.
4. Murray Michael F., Nicotinamide: An Oral Antimicrobial Agent with Activity against Both Mycobacterium tuberculosis and Human Immunodeficiency Virus, Clinical Infectious Diseases, 2003, 36, 453-460.
5. Yamaguchi T., Matsumura Y., Ishii T., Tokuoka Y., Kurita K., Synthesis of nicotinamide derivatives having a hydroxyl-substituted benzene ring and the influence of their structures on the apoptosis-inducing activity against leunkemia cells, Drug Development Rsearch, 2011, 72(3), 289-97.
6. Gozde Aydogan and Mehtap Kutlu., Biologia 2007, 62, 6-12.
7. Sharma D, Narasimhan B, Kumar P, Judge V, Narang R, De Clercq E, and Balzarini J., European journal of medicinal chemistry, 2009, 44(6), 2347-53.
8. Katsuhisa Uchida, Yayoi Nishiyama and Hideyo Yamaguchi., Journal of Infection and Chemotherapy, 2004, 10, 216-9.
9. H. Terauchi, A. Tanitame, K. Tada, K. Nakamura, Y. Seto and Y. Nishikawa, J. Med. Chem., 40(1997) 313.
10. Shekhar H, Pandey KB and Kant V Thermodynamic Characteristics of 1:2 molecular complex of Phthalic anhydride-Camphene system, J. Nat. Acd. Sci. Letter 2010; 33: 153-60.
11. Agrwal T, Gupta P, Das SS, Gupta A and Singh NB Phase equilibria crystallization and microstructural syudies of Naphthalen-2-ol + 1,3-Dinitrobenzene, J. Chem. Engg. Data 2010; 55: 4206-10.
12. Shekhar H. and Salim S. S., Molecular interactions and stability in binary organic alloys, J. Nat. Acad. Sci Letter, 2011, 34, 117-25.
13. Dwivedy Y., Kant S., Rai U. S. and Rai R. N., Synthesis, Physicochemical and Optical Characterization of Novel Fluorescing Complex: o-Phenylenediamine-Benzoin, Journal of Fluorescence, 2011, 21, 1255-63.
14. Shekhar H and Kant V Kinetic and Interfacial Studies on Transparent Organic Alloys, I. J. Chem. Soc. 2011; 88: 947-52.
15. Shamsuddin M., Singh S. B. and Nasar A., Thermodynamic investigations of liquid gallium-cadmium alloys, Thermochemica Acta, 1998, 316, 11-9.
16. Sharma B. L., Tandon S. and Gupta S., Characteristics of the binary faceted eutectic; benzoic Acid-Salicylic Acid system, Cryst. Res. Technol, 2009, 44, 258-68.
17. Nieto R., Gonozalez M. C., Herrero F., Thermodynamics of mixtures, functions of mixing and excess functions, American Journal of Physics, 1999, 67, 1096-9.
18. Agrwal T., Gupta P., Das S. S., Gupta A. and Singh N. B., Phase equilibria crystallization and microstructural syudies of Naphthalen-2-ol + 1,3-Dinitrobenzene, J. Chem. Engg. Data, 2010, 55, 4206-10.
19. J. D. Hunt, K. A. Jackson, Trans. Metall. Soc. AIME, 236(1966) 843.
20. Singh N. B., Glicksman M. E., Determination of the mean solid-liquid interface energy of pivalic acid, J. Cryst. Growth, 1989, 98, 573-80.
21. Turnbull D., Formation of crystal nuclei in liquid metals, J. Chem. Phys., 1950, 18, 768.
22. J. D. Hunt and S. Z. Lu, Hand Book of Crystal Growth (1994) Ed. DTJ Hurle, Elsevier, Amsterdam p.112.
23. G. A. Chadwick, Metallography of Phase Transformation, 1972, Butterworths, London, p.61
24. Wilcox W. R., The relation between classical nucleation theory and the solubility of small particles, Journal of crystal growth, 1974, 26, 153-154.
25. M. Gunduz, J. D. Hunt, Acta Metall., 37(1989), 1839.
26. Y. Ocak, S. Akbulut, K. Keslioglu, N. Marasli, Journal of Colloid and Interface Science, 320(2008) 555.

****